8 - SISTEMAS PERITÉTICOS BINÁRIOS

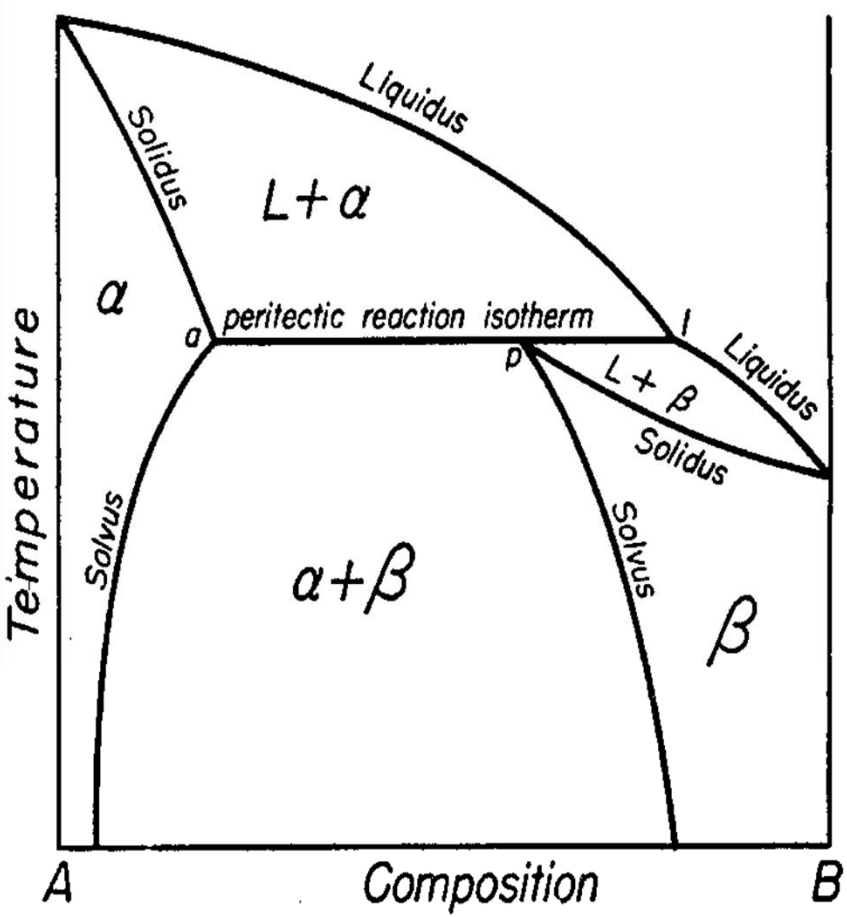

FIG. 8-1

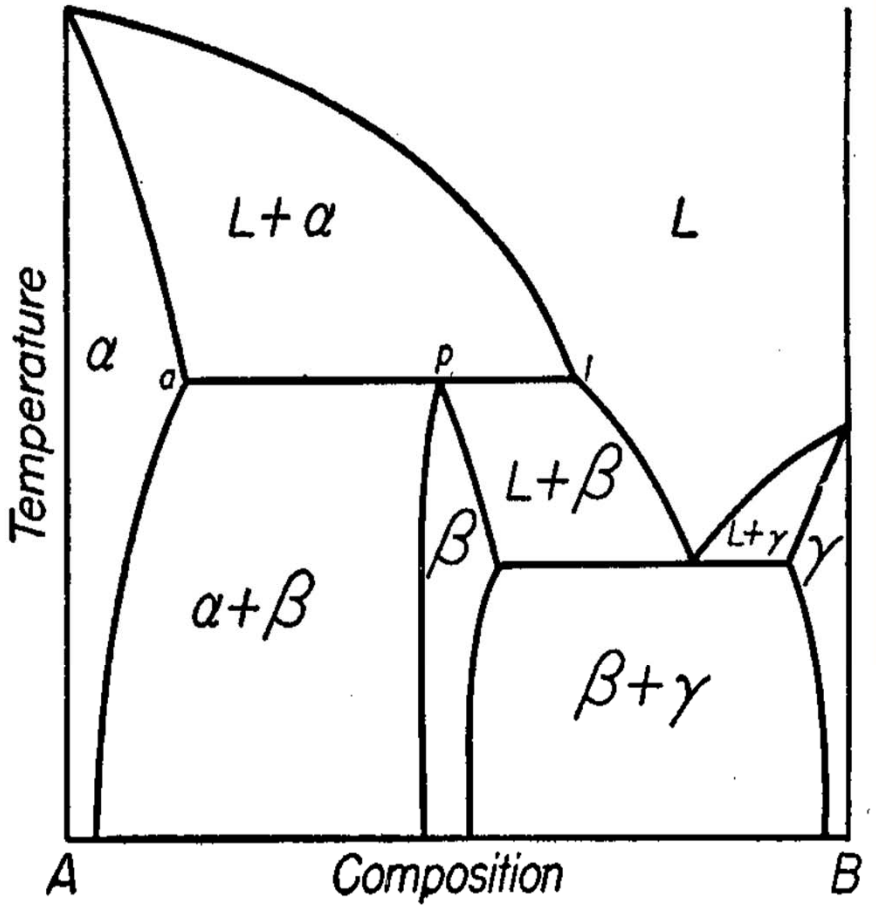

FIG. 8-2

$$\alpha + L \underset{\text{aquecimento}}{\overset{\text{resfriamento}}{\rightleftharpoons}} \beta$$

Ni-Re

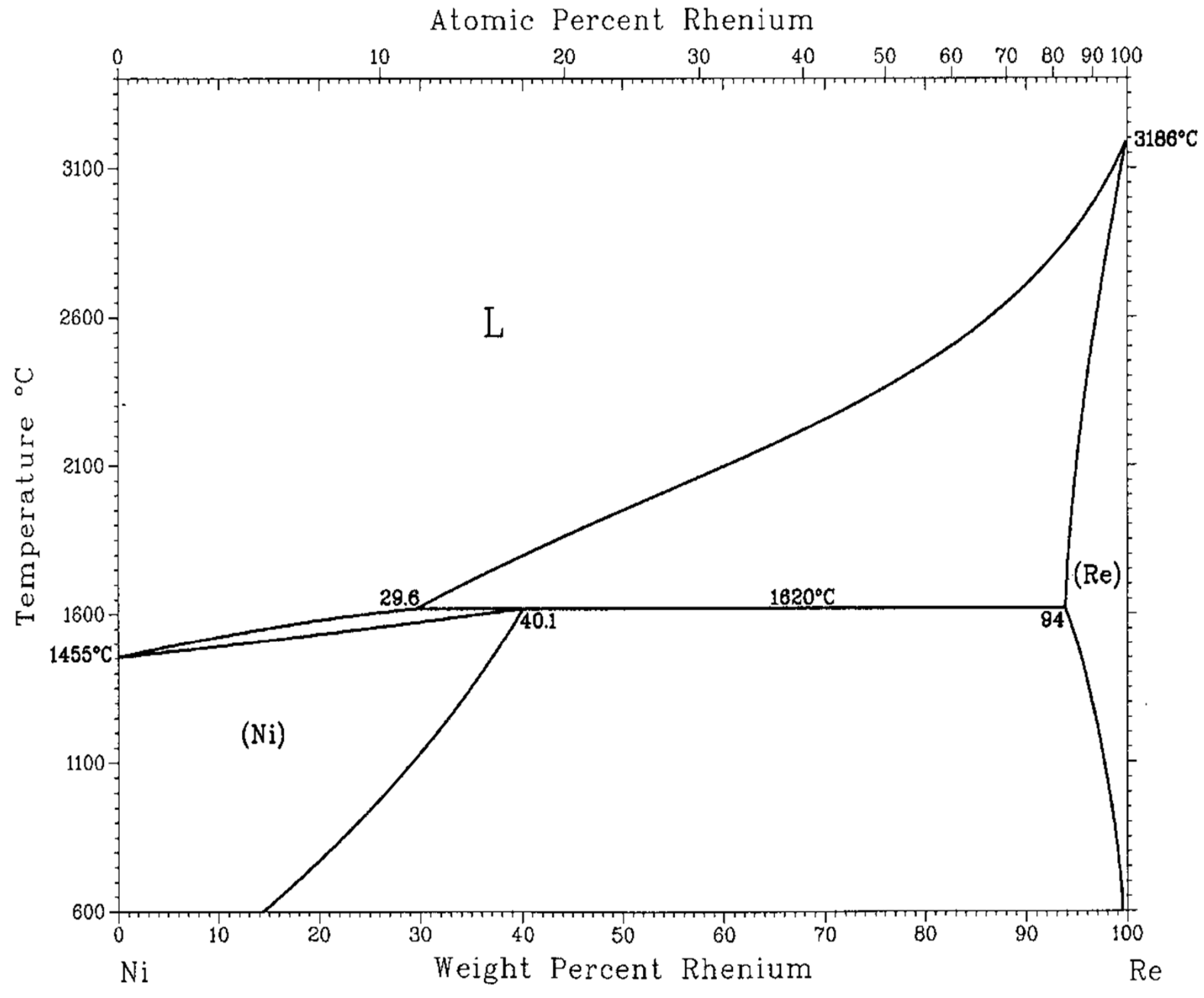
Atomic Percent Rhenium
0
10
20
30
40
50
60
70
80
90
100
3186°C
3100
2600
2100
1600
1100
600
Temperature °C
L
29.6
1620°C
40.1
94
1455°C
(Re)
(Ni)
0
10
20
30
40
50
60
70
80
90
100
Ni
Weight Percent Rhenium
Re

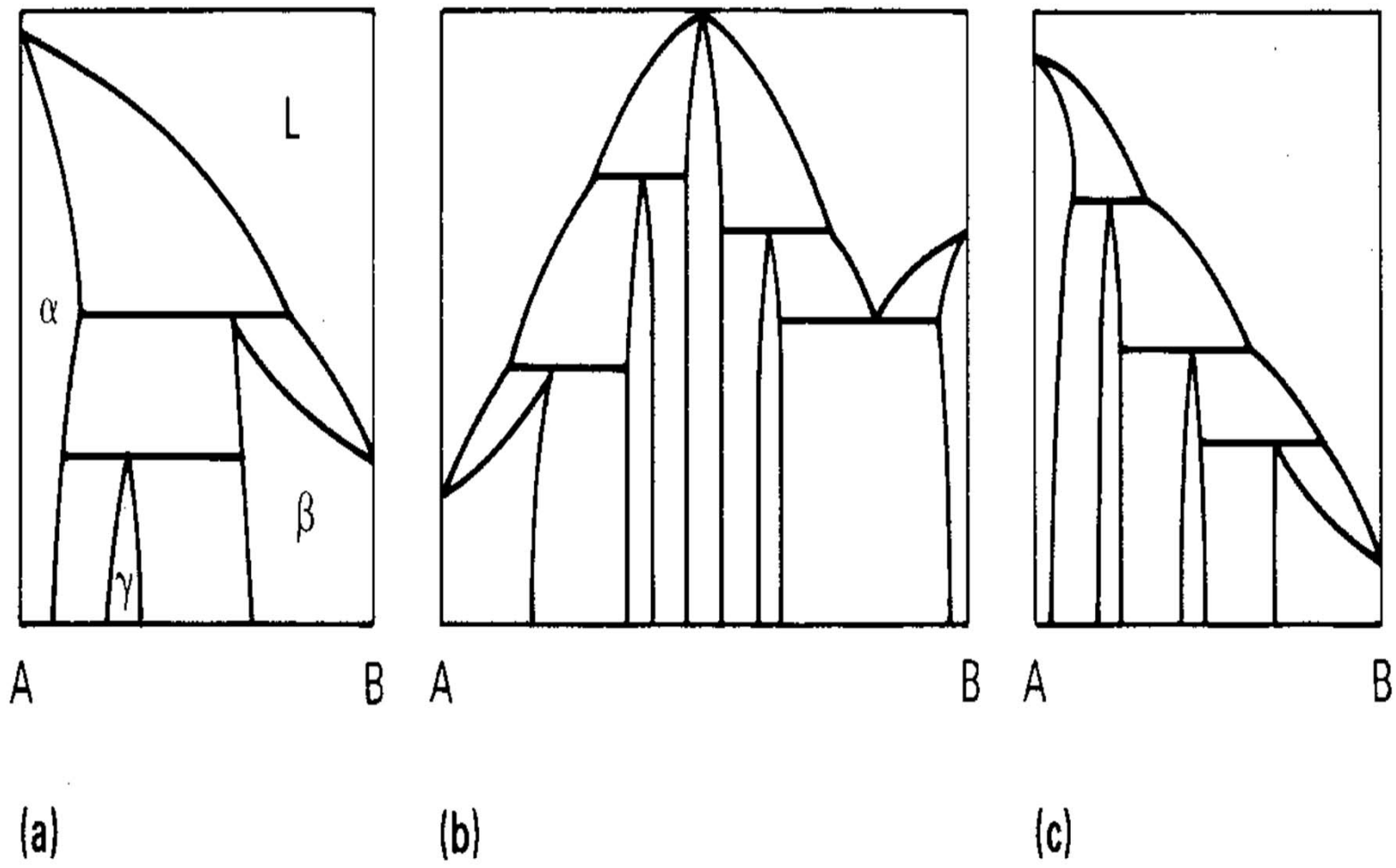

Fig. 1 Typical peritectic phase diagrams. (a) Peritectic reaction α + liquid $\rightarrow \beta$ and peritectoid reaction $\alpha + \beta \rightarrow \gamma$. (b) Peritectic formation of intermetallic phases from a high-melting intermetallic. (c) Peritectic cascade between high- and low-melting components.

Al-Cr

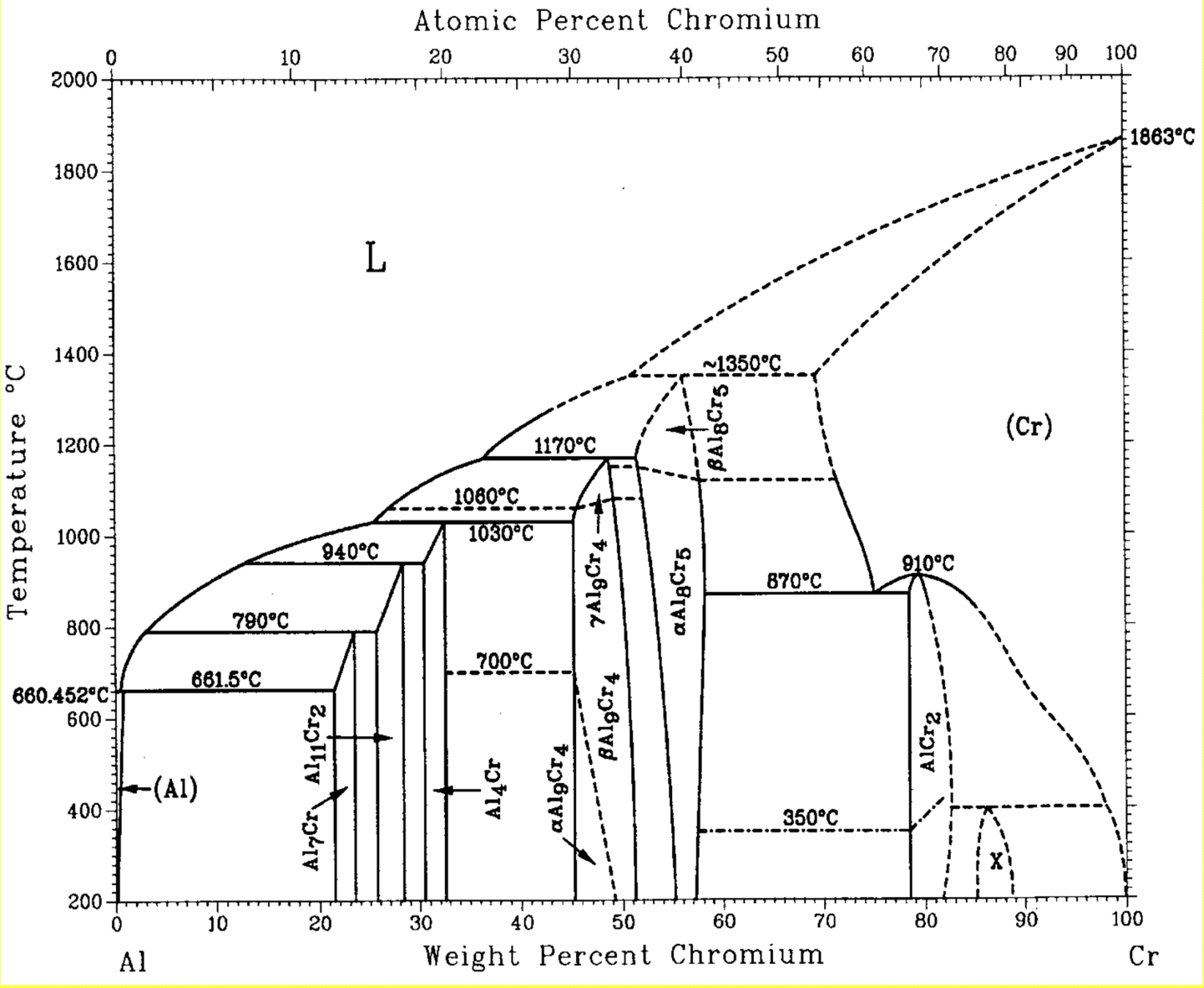
Atomic Percent Chromium
0
10
20
30
40
50
60
70
80
90
100
2000
1800
1600
1400
1200
1000
800
600
400
200
Temperature °C
L
(Cr)
1863°C
1350°C
1170°C
1060°C
1030°C
940°C
790°C
700°C
661.5°C
660.452°C
870°C
910°C
350°C
(Al)
Al11Cr2
Al7Cr
Al4Cr
αAl8Cr4
βAl8Cr4
γAl8Cr4
αAl8Cr5
βAl8Cr5
AlCr2
X
Al
Weight Percent Chromium
Cr

8.1 - Resfriamento em equilíbrio

Liga de composição peritética

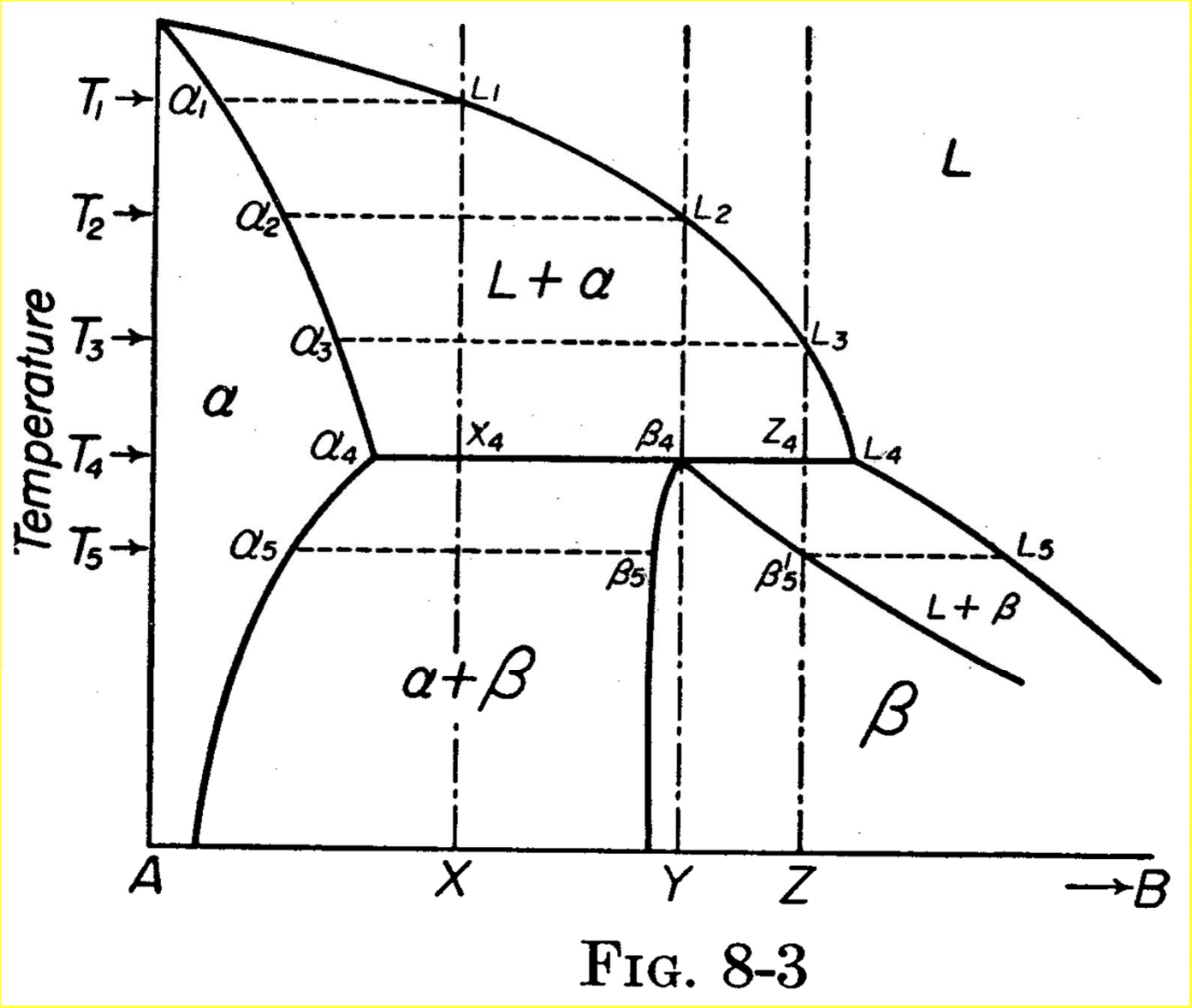

FIG. 8-3

$\alpha + L \underset{\text{aquecimento}}{\overset{\text{resfriamento}}{\rightleftharpoons}} \beta$

% L=

% α_p=

8.2 - Resfriamento fora de equilíbrio

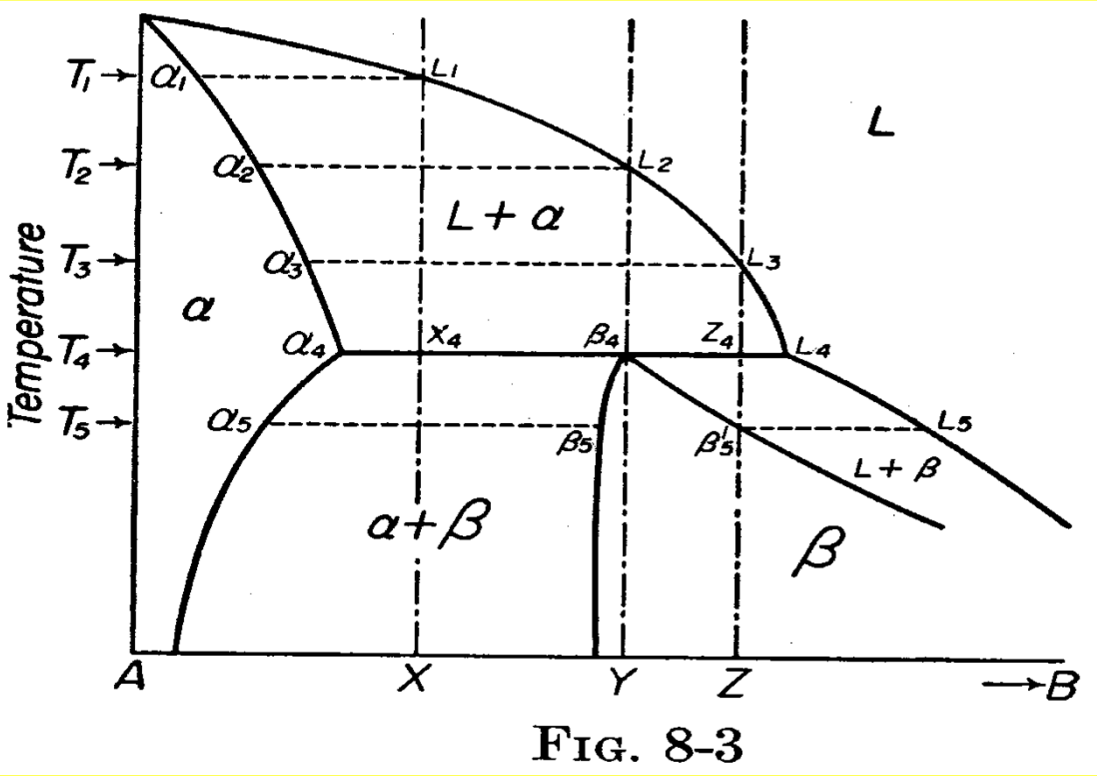

FIG. 8-3

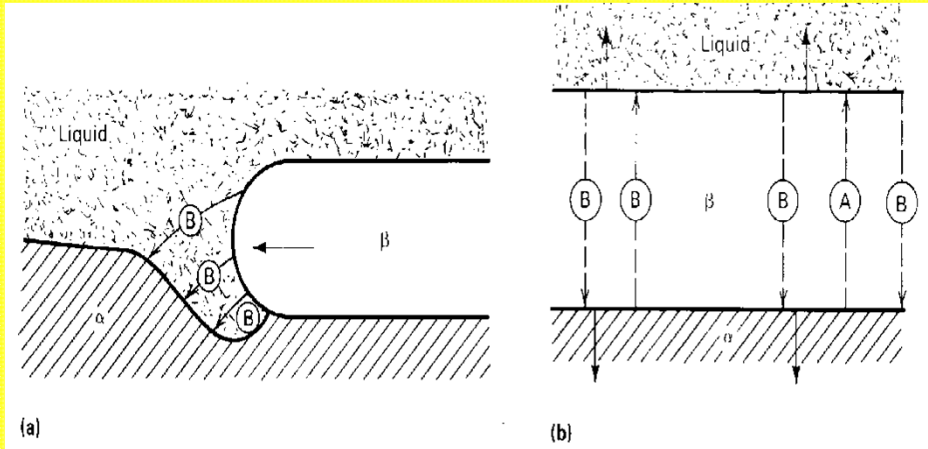

Fig. 2 Mechanisms of peritectic reaction and transformation. (a) Lateral growth of a β layer along the α/liquid interface during peritectic reaction by liquid diffusion. (b) Thickening of a β layer by solid-state diffusion during peritectic transformation. The solid arrows indicate growth direction of β; dashed arrows, the diffusion of the atomic species. (Ref 11)

Cu-Sn

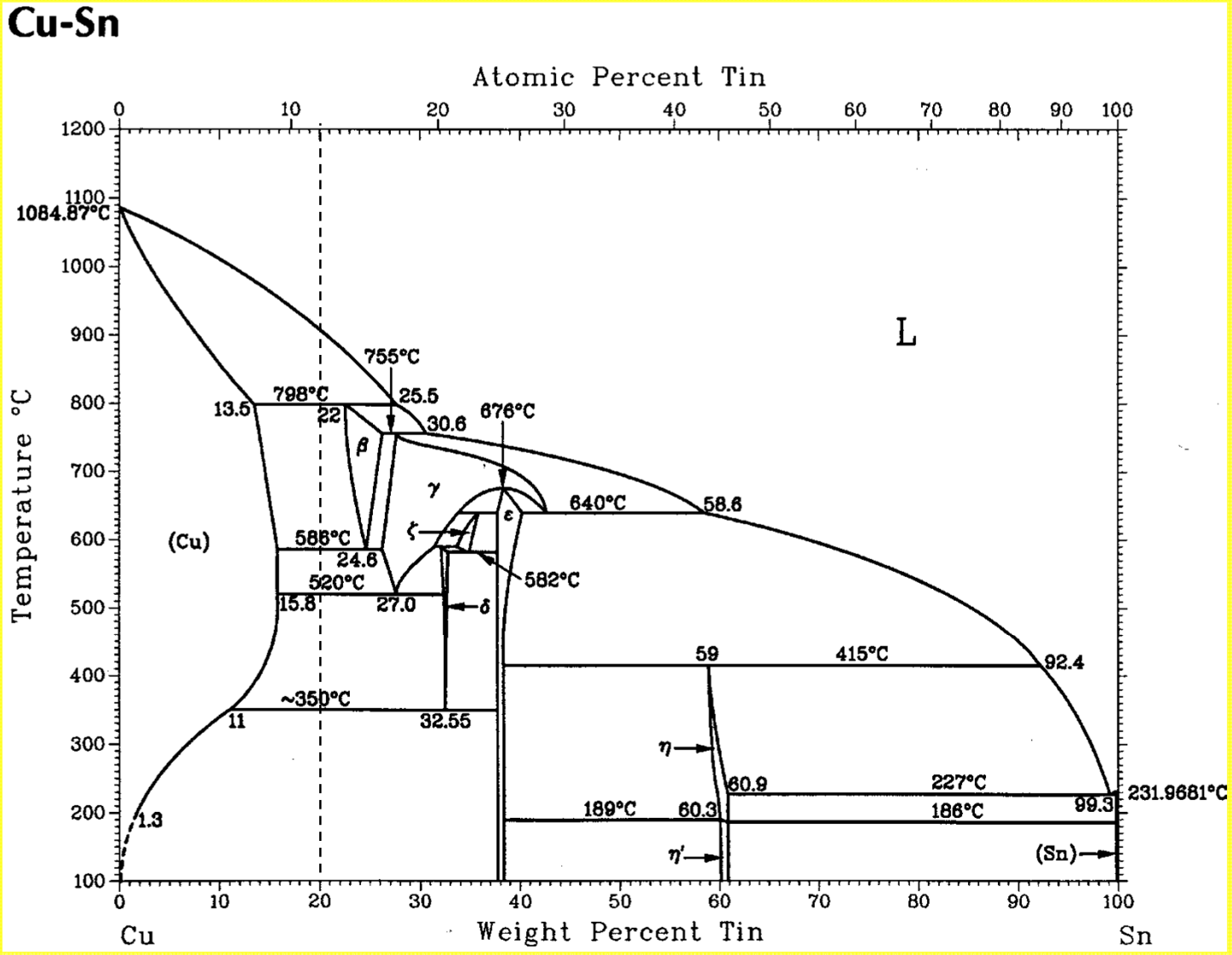

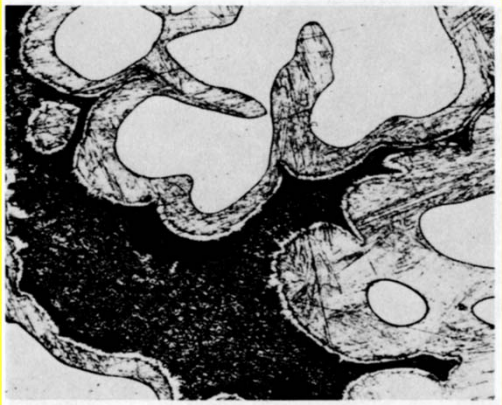

Fig. 9 Start of the peritectic transformation in the same directionally solidified Cu-20Sn alloy shown in Fig. 7, but at higher magnification. Note the homogeneous thickness of the β layers (gray) around the primary α (white). The matrix (dark) is a mixture of tin-rich phases. Mechanically polished, etched in HNO_3. 160×. (Ref 6)

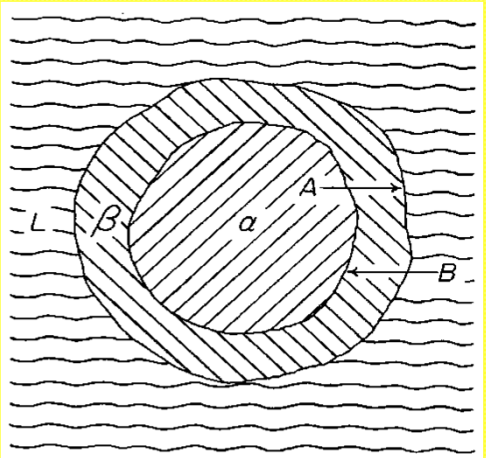

FIG. 8-4. Schematic representation of primary α undergoing peritectic reaction with liquid L to form an envelope of β. The reaction progresses by the diffusion of A atoms outward and B atoms inward through the shell of β.

Cd-Cu

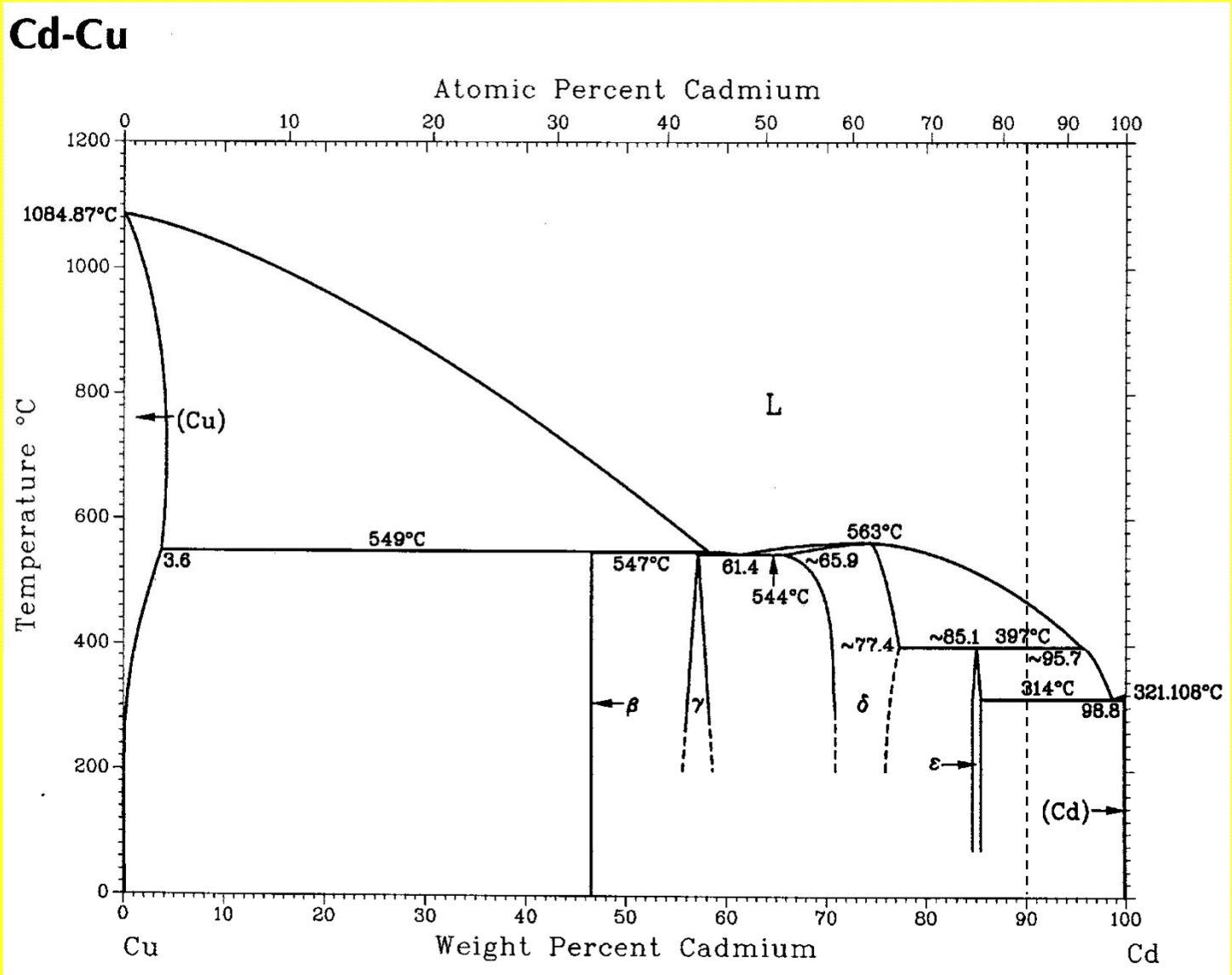

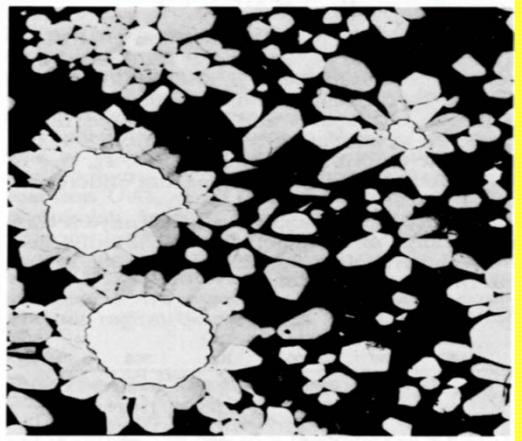

Fig. 15 Microstructure of a Cd-10Cu alloy that was cooled to 410 °C (770 °F) and held 20 h, then cooled to 305 °C (580 °F) and held 160 min (peritectic temperature: 397 °C, or 747 °F). Note the faceted coarse crystals of the peritectically formed $CuCd_3$ envelopes (gray). The primary Cu_5Cd_8 crystals are white; the dark matrix is cadmium. Mechanically polished, etched in HNO_3. 100×

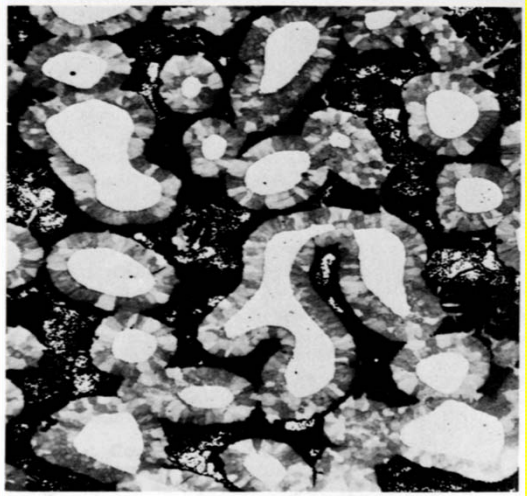

Fig. 16 Same as Fig. 15, except alloy was cooled to 410 °C (770 °F) and held 20 h, then cooled to 275 °C (525 °F) and held 160 min (peritectic temperature: 397 °C, or 747 °F; eutectic temperature: 314 °C, or 597 °F). Note large number of grain boundaries in the peritectic $CuCd_3$ phase (gray) and its smooth interfaces with the primary Cu_5Cd_8 crystals (white) and the matrix Cd (dark). 100×

Au-Bi

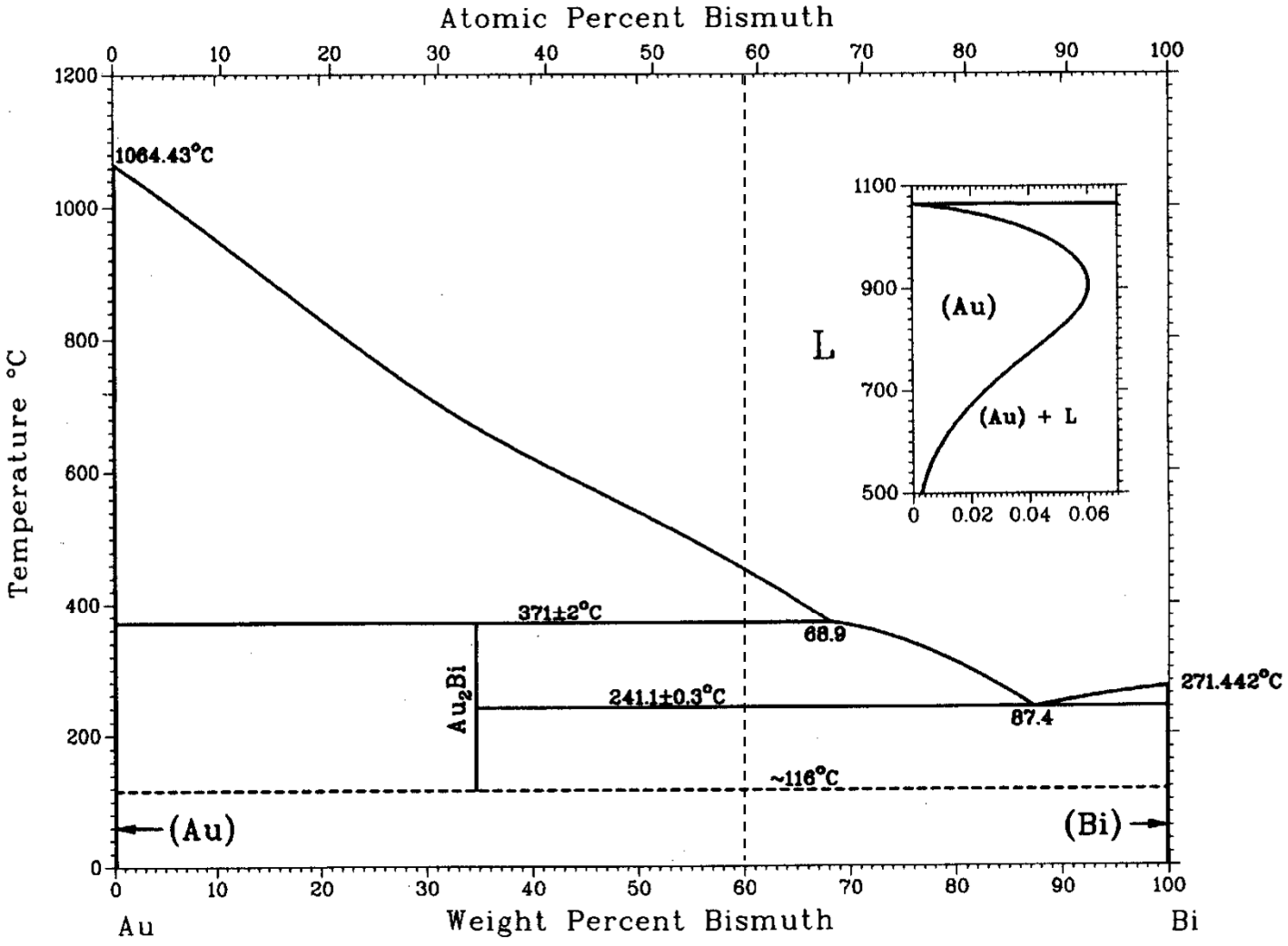

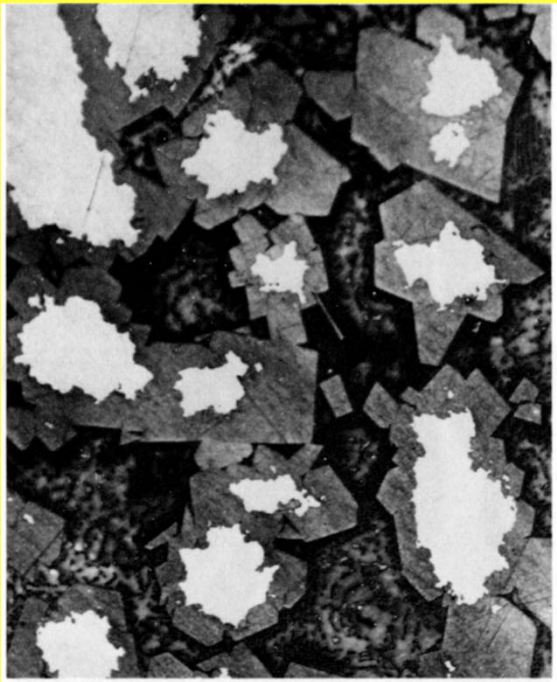

Fig. 18 Peritectic envelope in a Bi-40Au alloy that was cooled to 450 °C (840 °F) and held 5 h, then cooled to 300 °C (570 °F) and held 2 h (peritectic temperature: 373 °C, or 703 °F). The morphology is entirely determined by the anisotropy of the interfacial energy of the face-centered cubic Au_2Bi crystals (gray). The primary crystals are gold (white); the matrix is the Au_2Bi-Bi eutectic. Mechanically polished, contrasted by reactively sputtered interference layer. 200×

Al-U

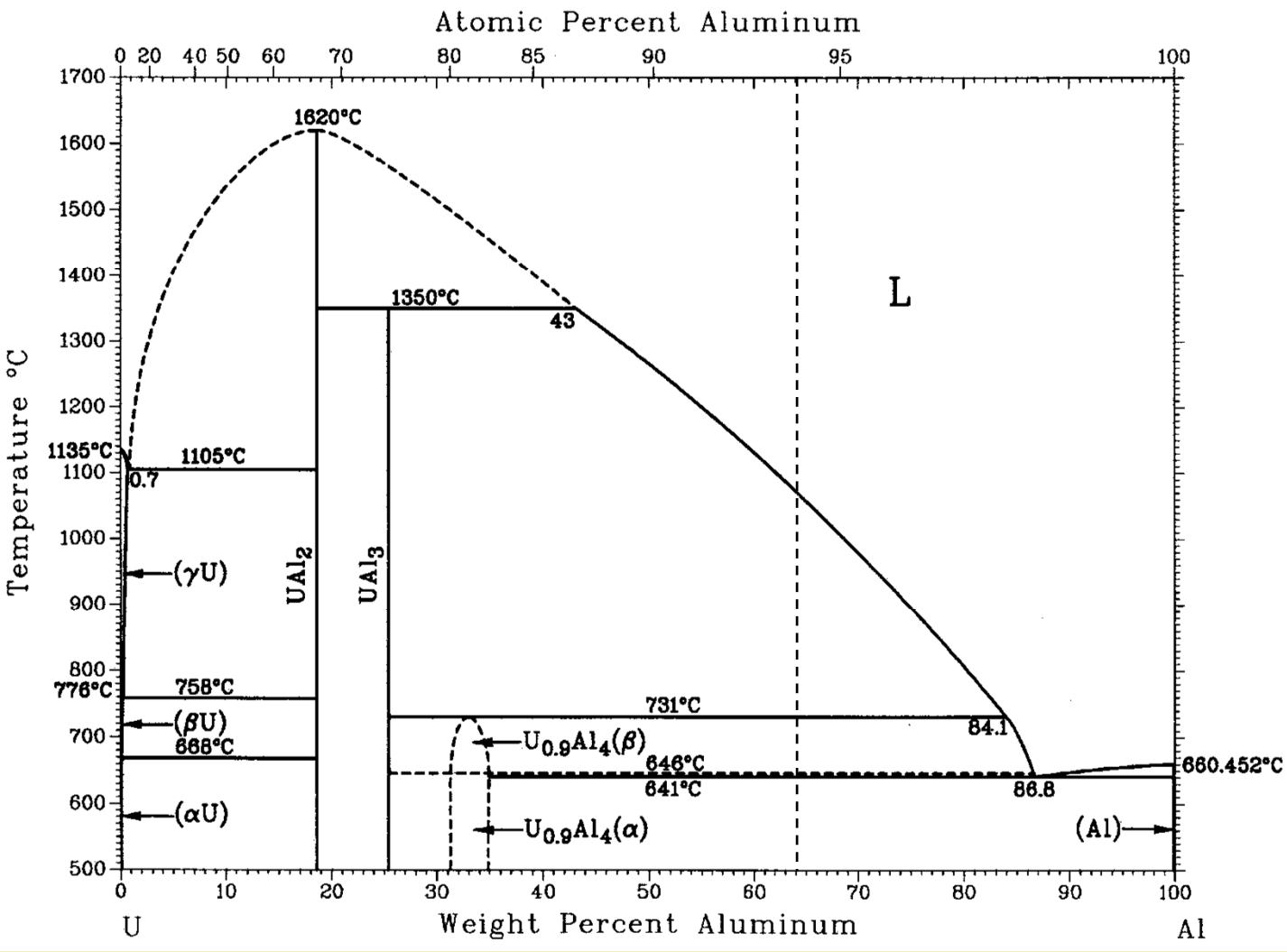

Fig. 3 Primary UAl_3 (gray) partially surrounded by peritectically formed UAl_4 (dark) in an Al-6U alloy that was cooled slowly from above liquidus to 760 °C (1400 °F) and held 10 min, then cooled to 670 °C (1240 °F) and held 15 min (peritectic temperature: 732 °C, or 1350 °F). The matrix is aluminum (white) with UAl_4 (dark) eutectic. This $UAl_3 + Al \rightarrow UAl_4$ reaction leads to unfavorable rolling behavior. Electrolytically polished, etched in 50% HNO_3. 700×

Sistema V-Si

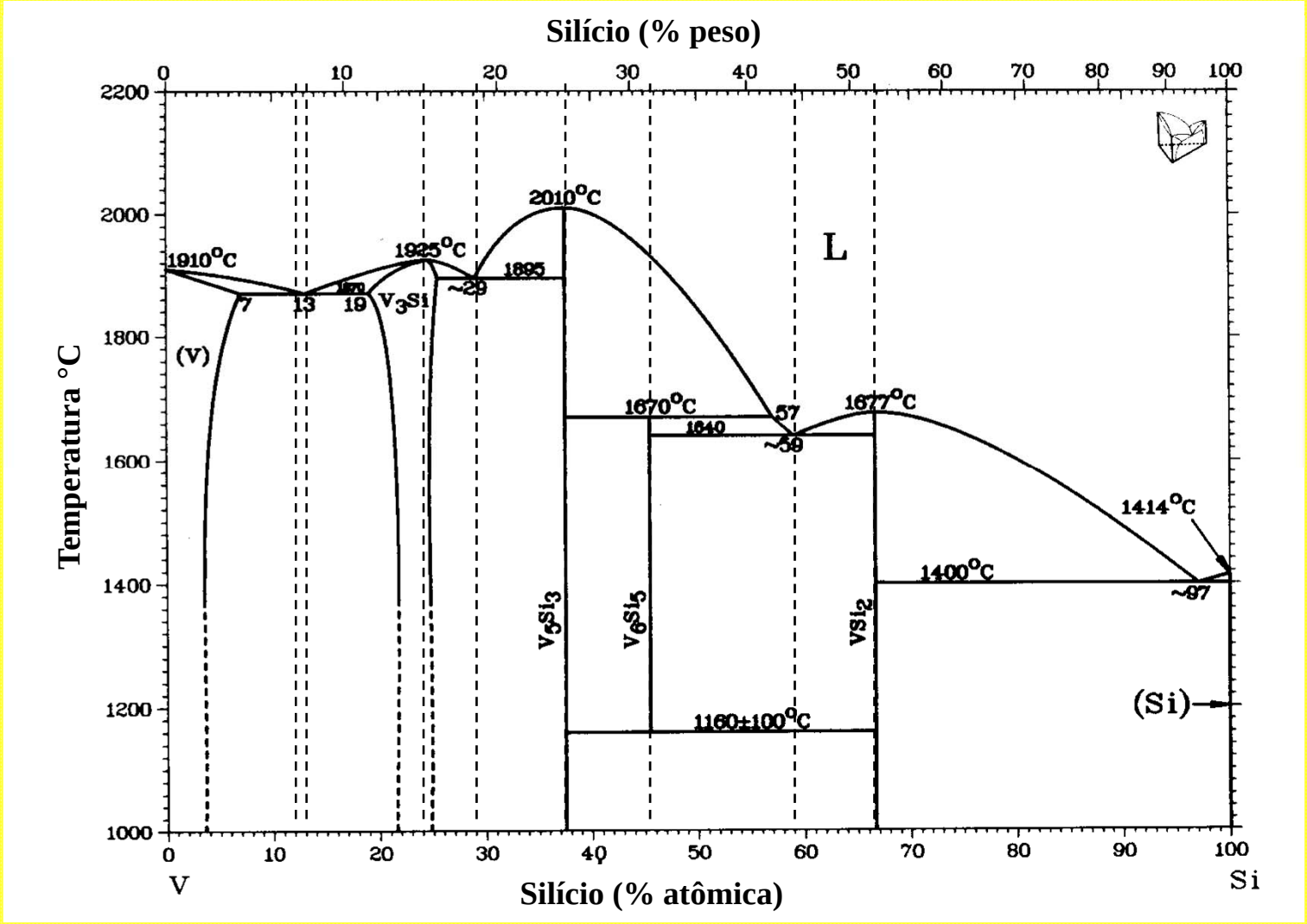

[1990Mas]

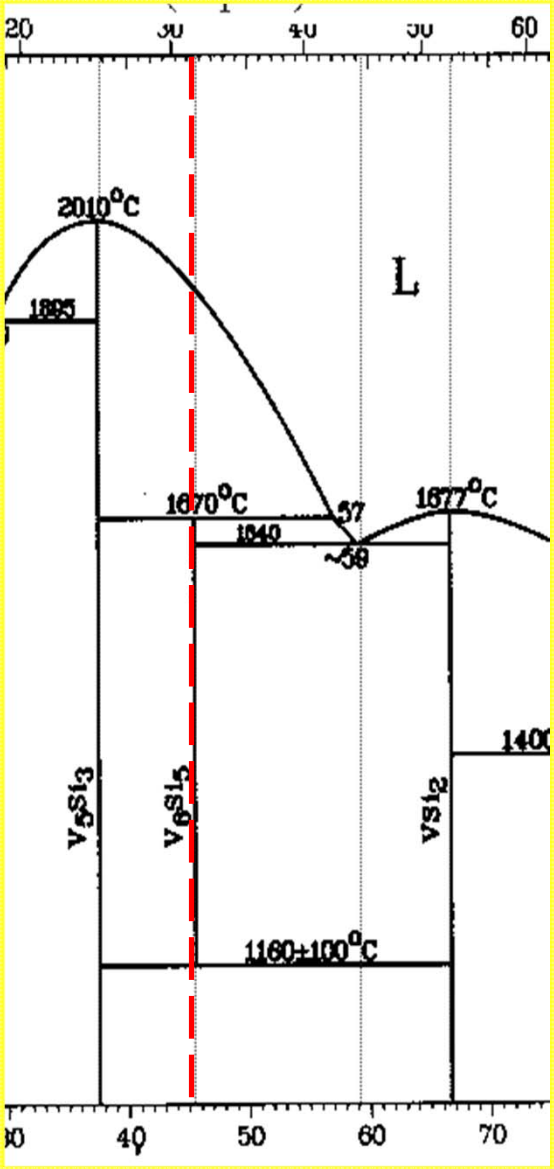
20
60
2010°C
L
1895
1670°C
57
1677°C
1640
~59
1400
V_5Si_3
V_6Si_5
VSi_2
1160±100°C
30
40
50
60
70

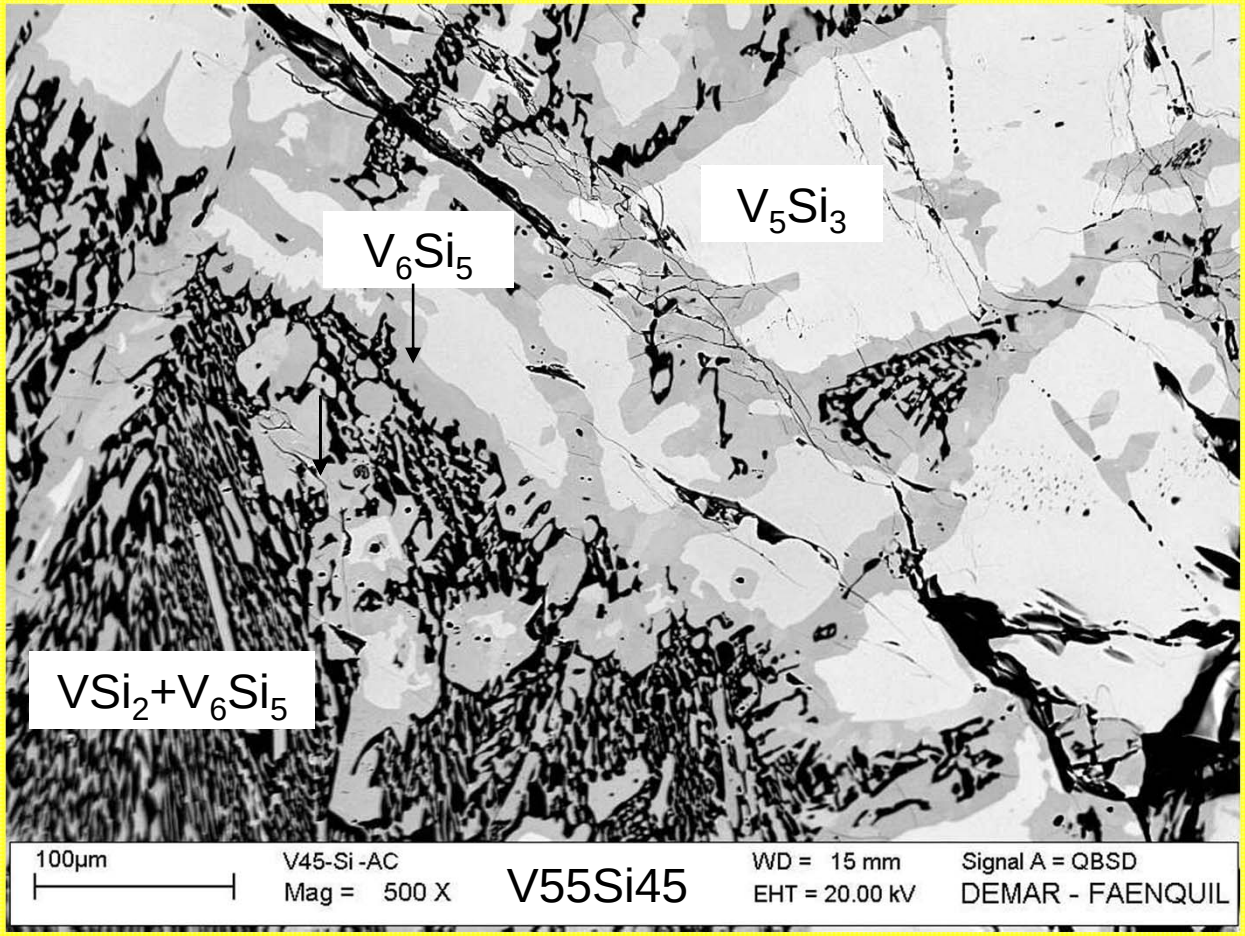
V_5Si_3
V_6Si_5
$VSi_2+V_6Si_5$
100µm
V45-Si -AC
Mag = 500 X
V55Si45
WD = 15 mm
EHT = 20.00 kV
Signal A = QBSD
DEMAR - FAENQUIL

[1990Mas]

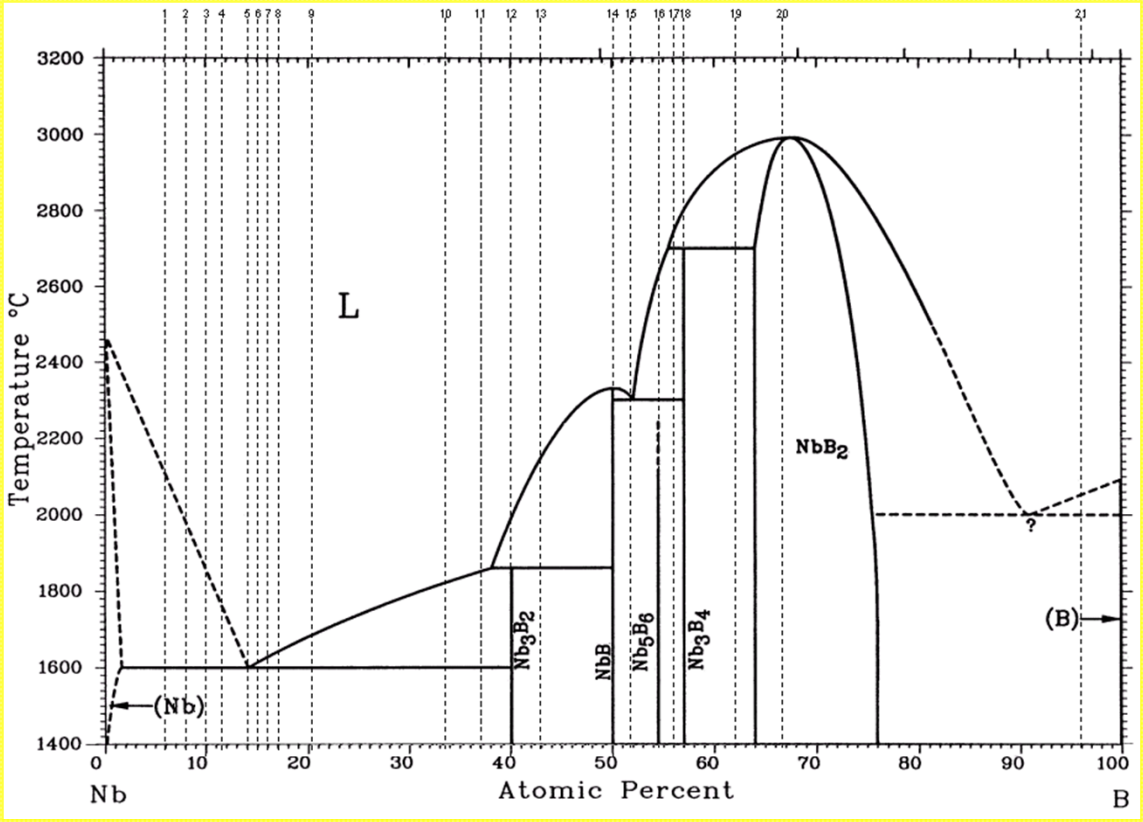
1 2 3 4 5 6 7 8 9 10 11 12 13 14 15 16 17 18 19 20 21
3200
3000
2800
2600
2400
2200
2000
1800
1600
1400
Temperature °C
L
NbB2
?
(B)
Nb3B2
NbB
Nb5B6
Nb3B4
(Nb)
0 10 20 30 40 50 60 70 80 90 100
Nb
Atomic Percent
B

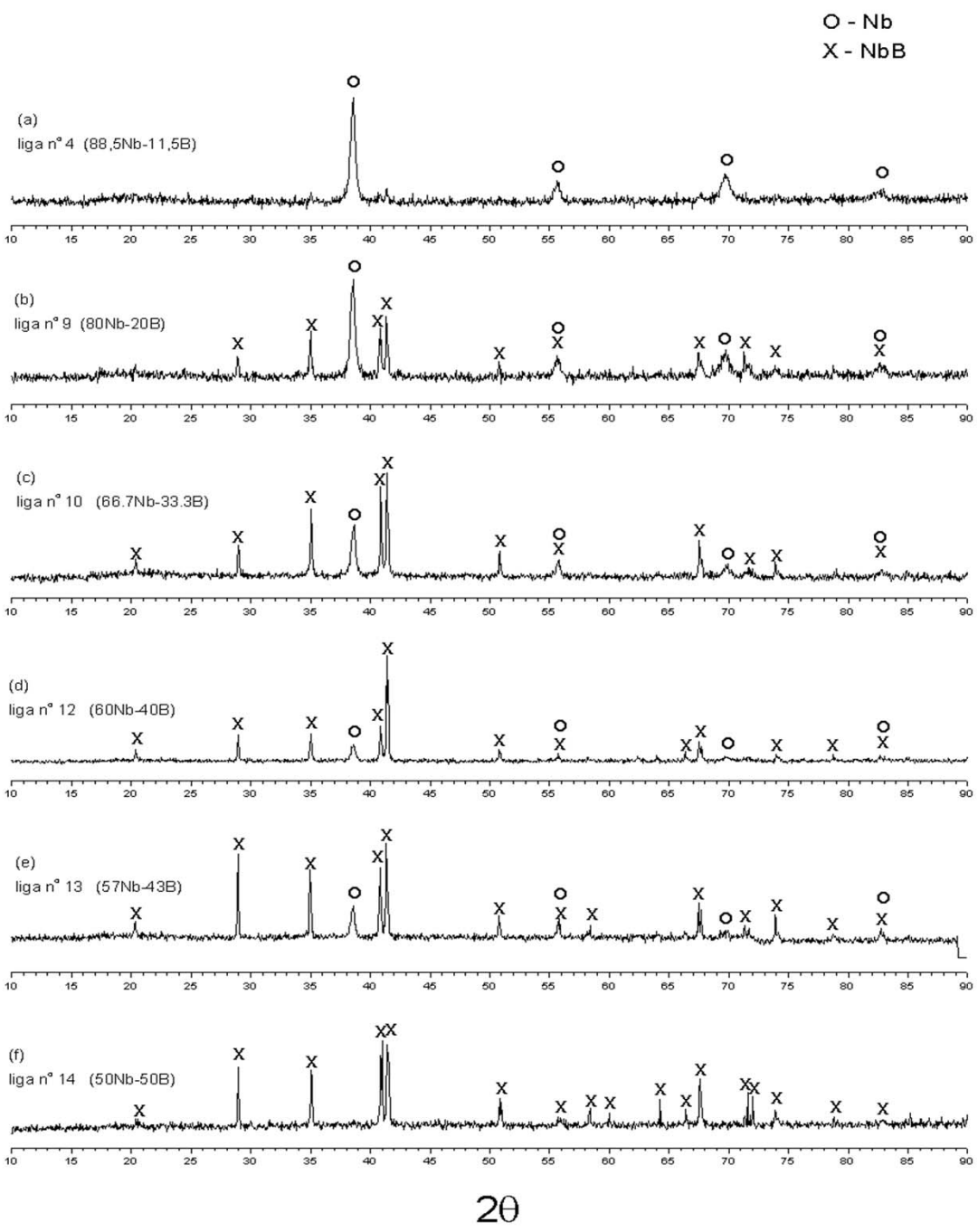
O - Nb
X - NbB
(a)
liga n° 4 (88,5Nb-11,5B)
(b)
liga n° 9 (80Nb-20B)
(c)
liga n° 10 (66.7Nb-33.3B)
(d)
liga n° 12 (60Nb-40B)
(e)
liga n° 13 (57Nb-43B)
(f)
liga n° 14 (50Nb-50B)
10 15 20 25 30 35 40 45 50 55 60 65 70 75 80 85 90
2θ

Amostra 44Nb56B

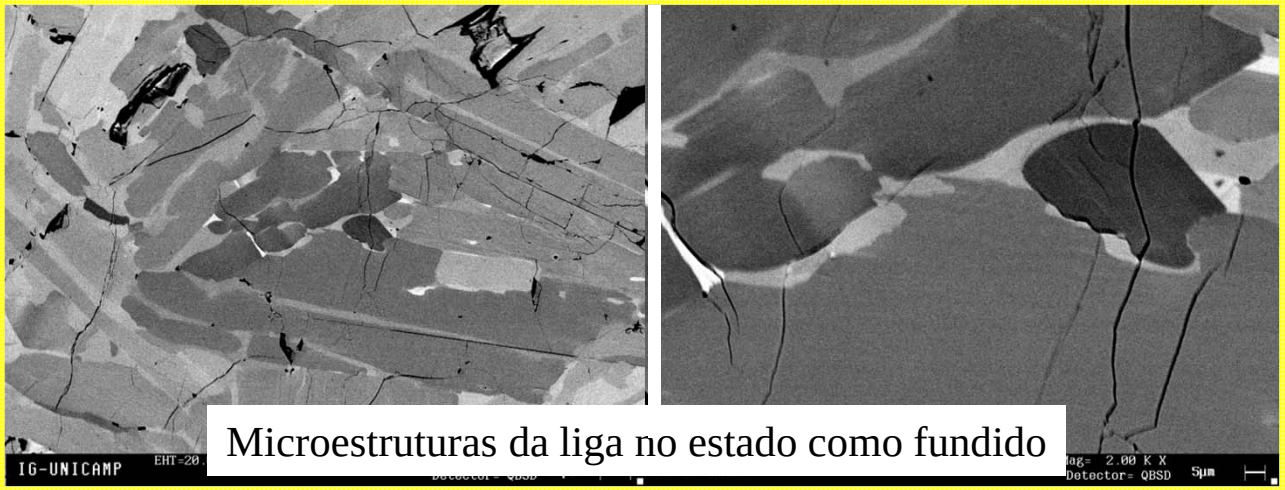

Microestruturas da liga no estado como fundido

XRD: NbB, Nb_5B_6 e Nb_3B_4

Amostra 42,9Nb57,1B

Microestruturas da liga no estado como fundido

XRD: Nb_3B_4 - picos intensos

NbB, NbB_2 - pq quantidade

Sistema Hf–B proposto por RUDY e WINDISCH (1966)

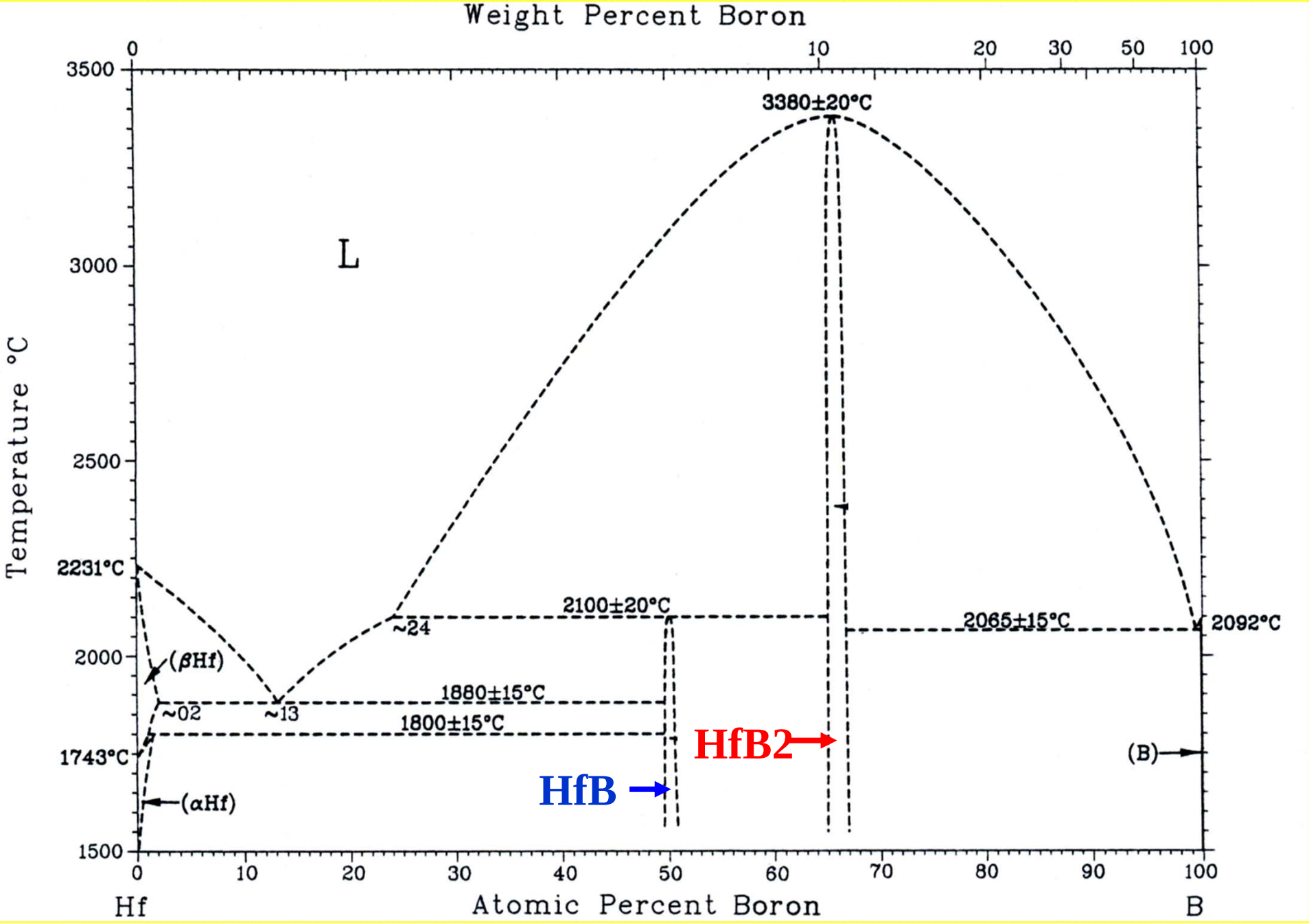

Liga Hf–B no estado bruto de fusão

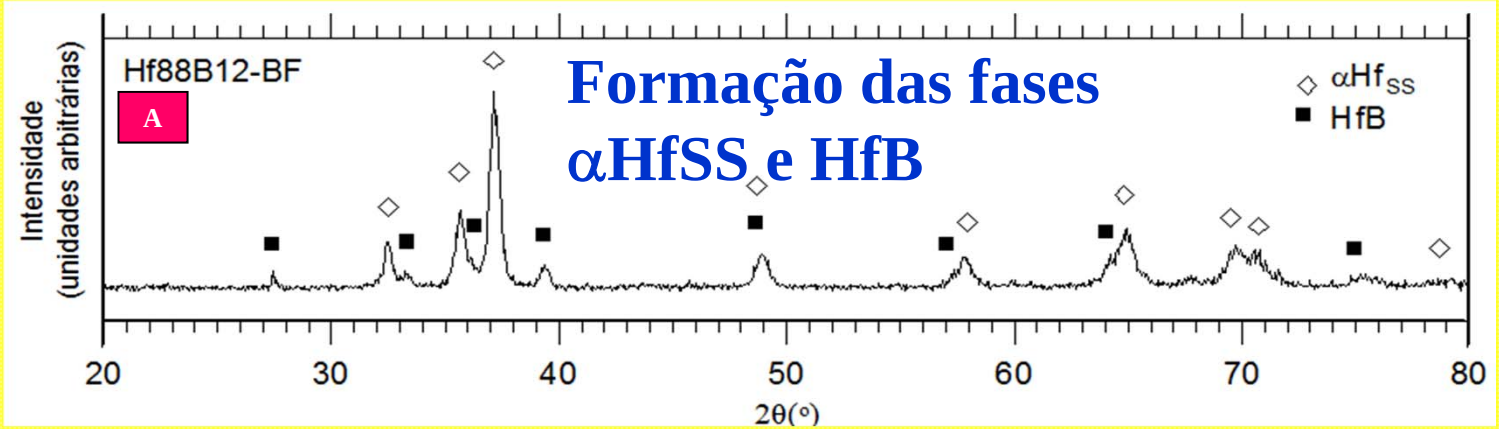

Formação das fases αHfSS e HfB

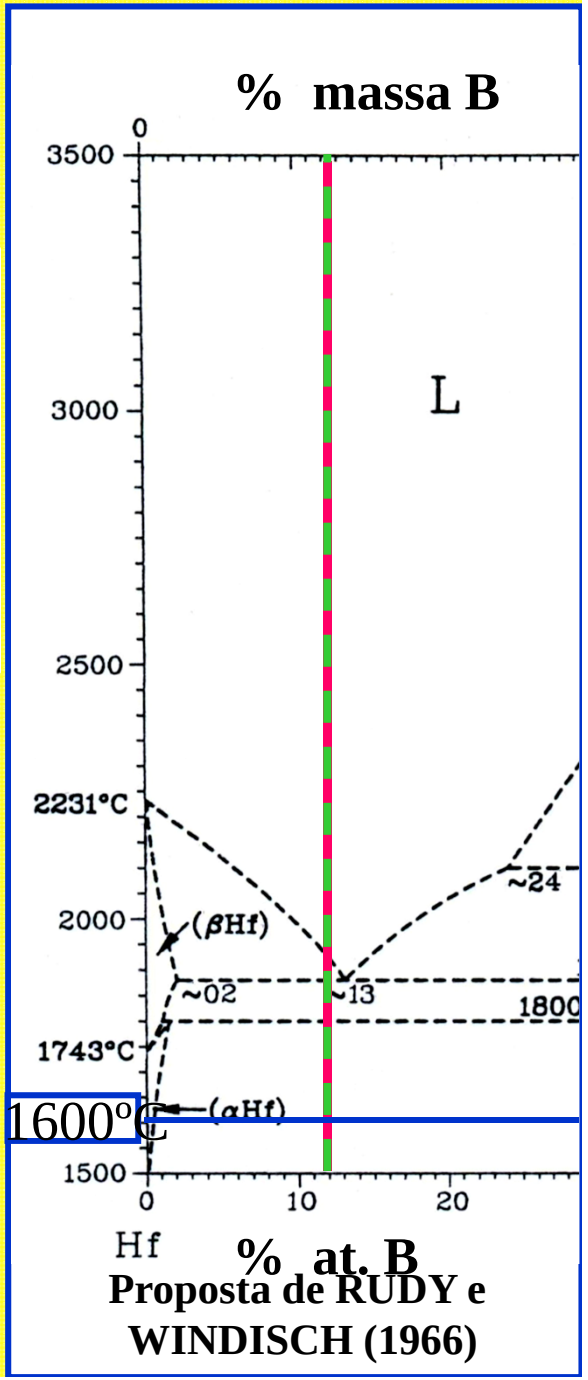

Proposta de RUDY e WINDISCH (1966)

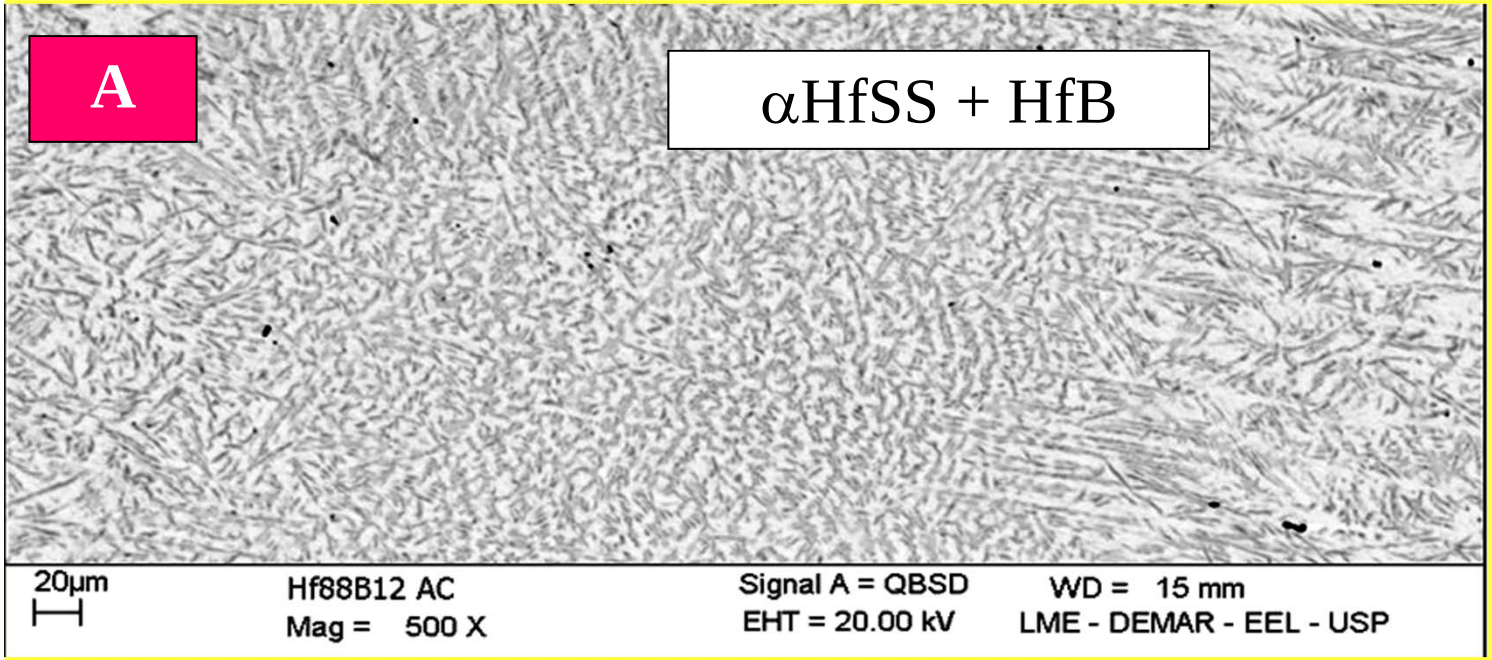
A
αHfSS + HfB
20µm
Hf88B12 AC
Mag = 500 X
Signal A = QBSD
EHT = 20.00 kV
WD = 15 mm
LME - DEMAR - EEL - USP

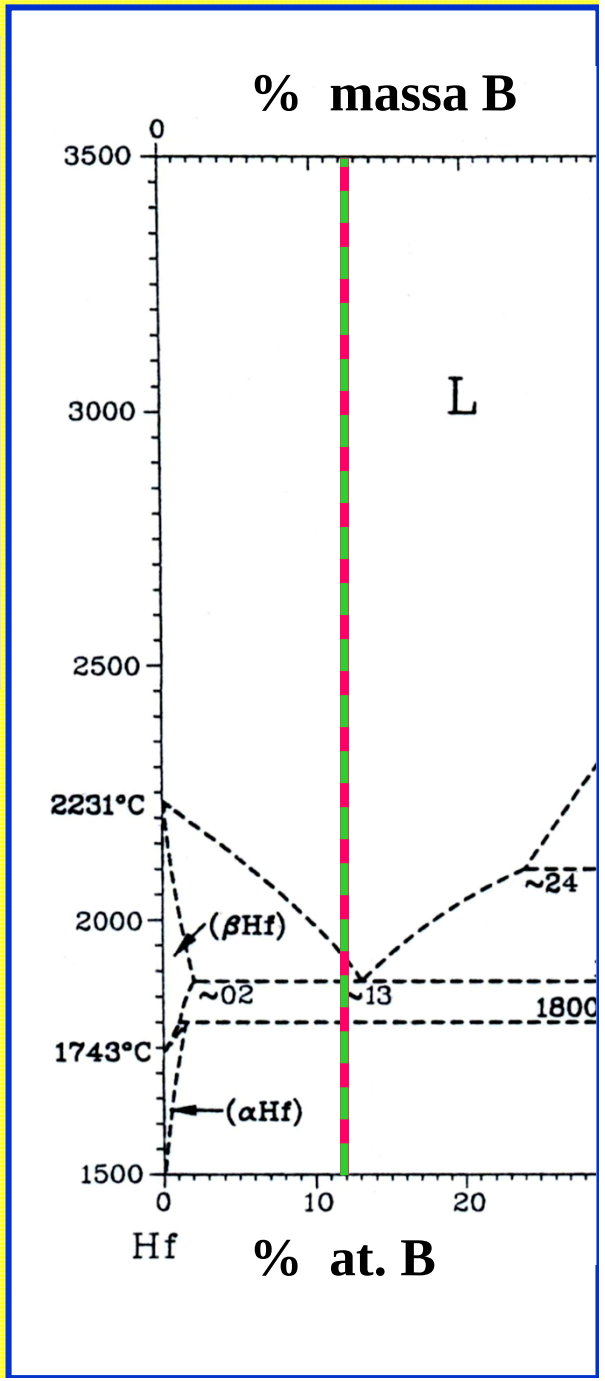
% massa B
0
3500
3000
2500
2231°C
2000
1743°C
1500
L
(βHf)
~02
~13
~24
1800
(αHf)
0
10
20
Hf
% at. B

Ligas Hf–B no estado bruto de fusão

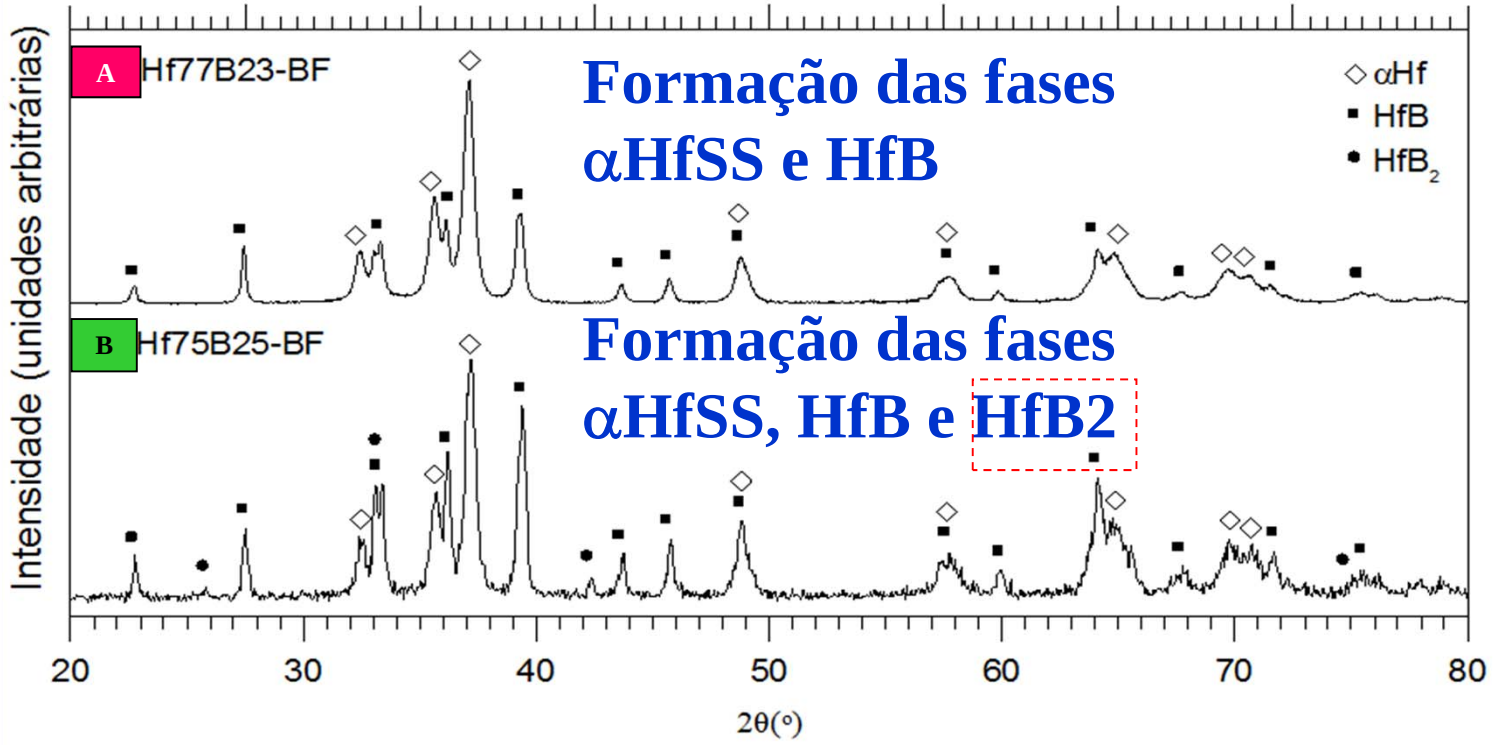

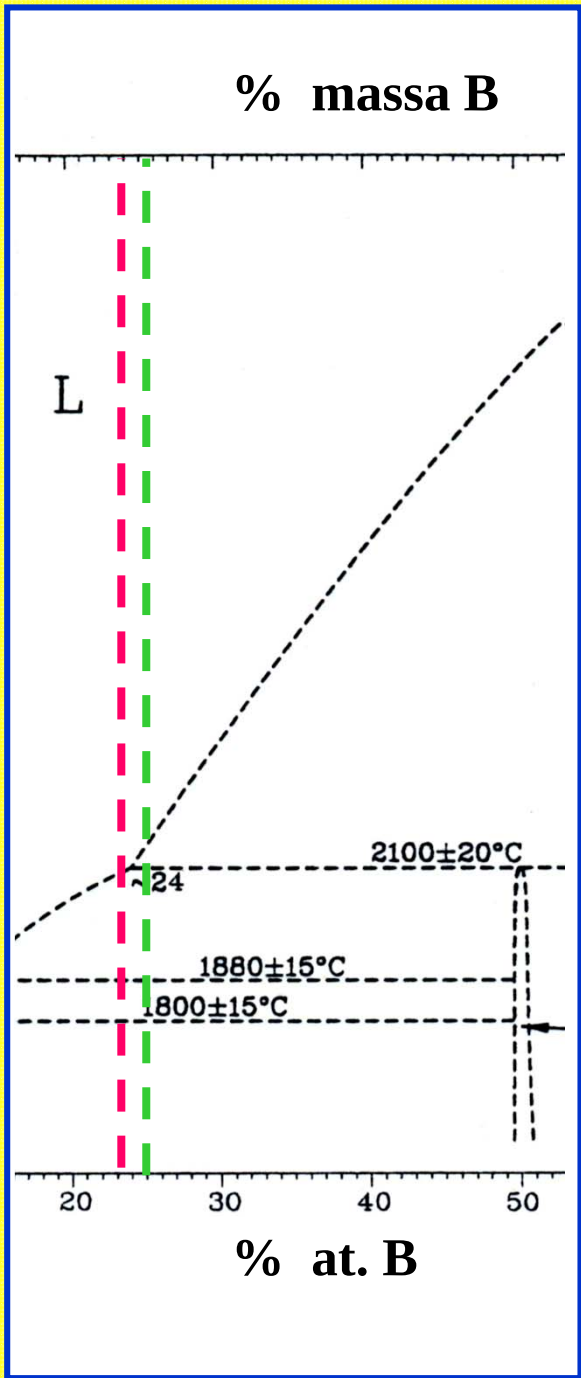

Ligas Hf–B no estado bruto de fusão

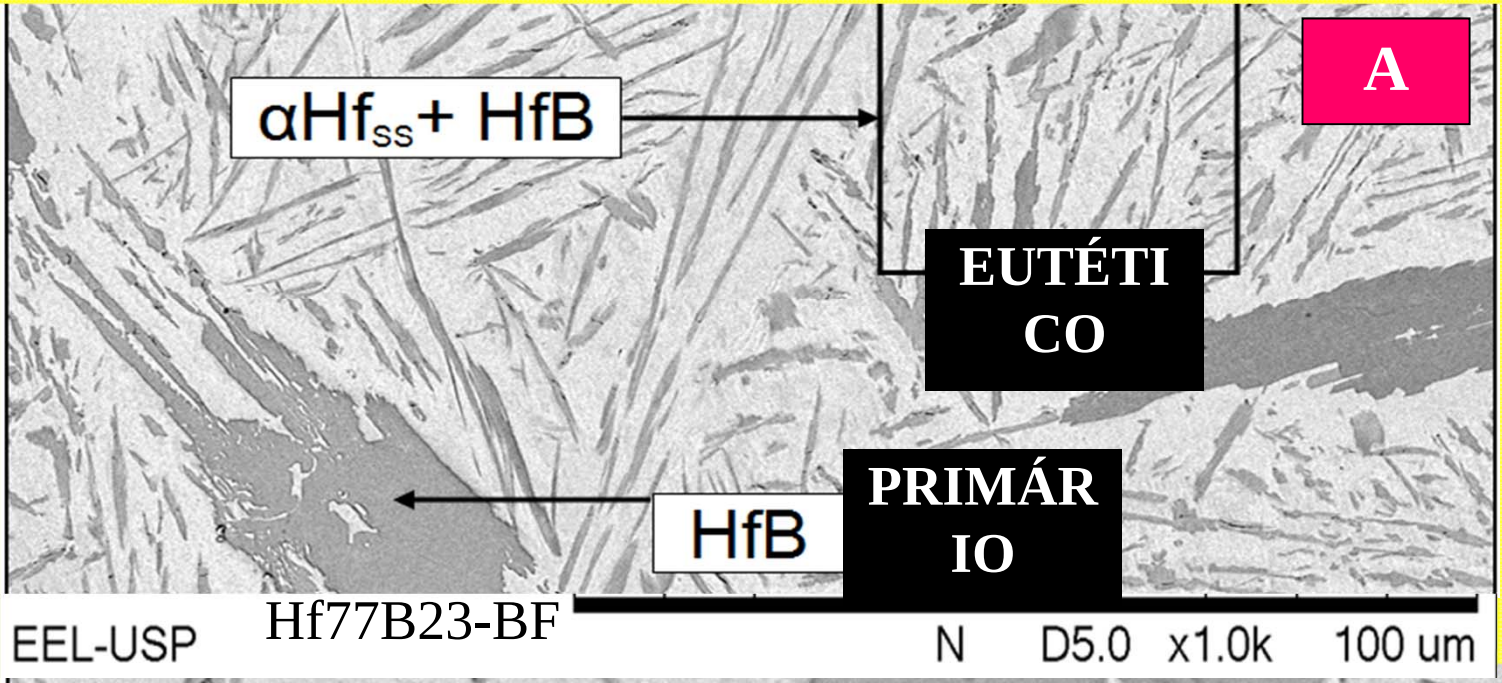

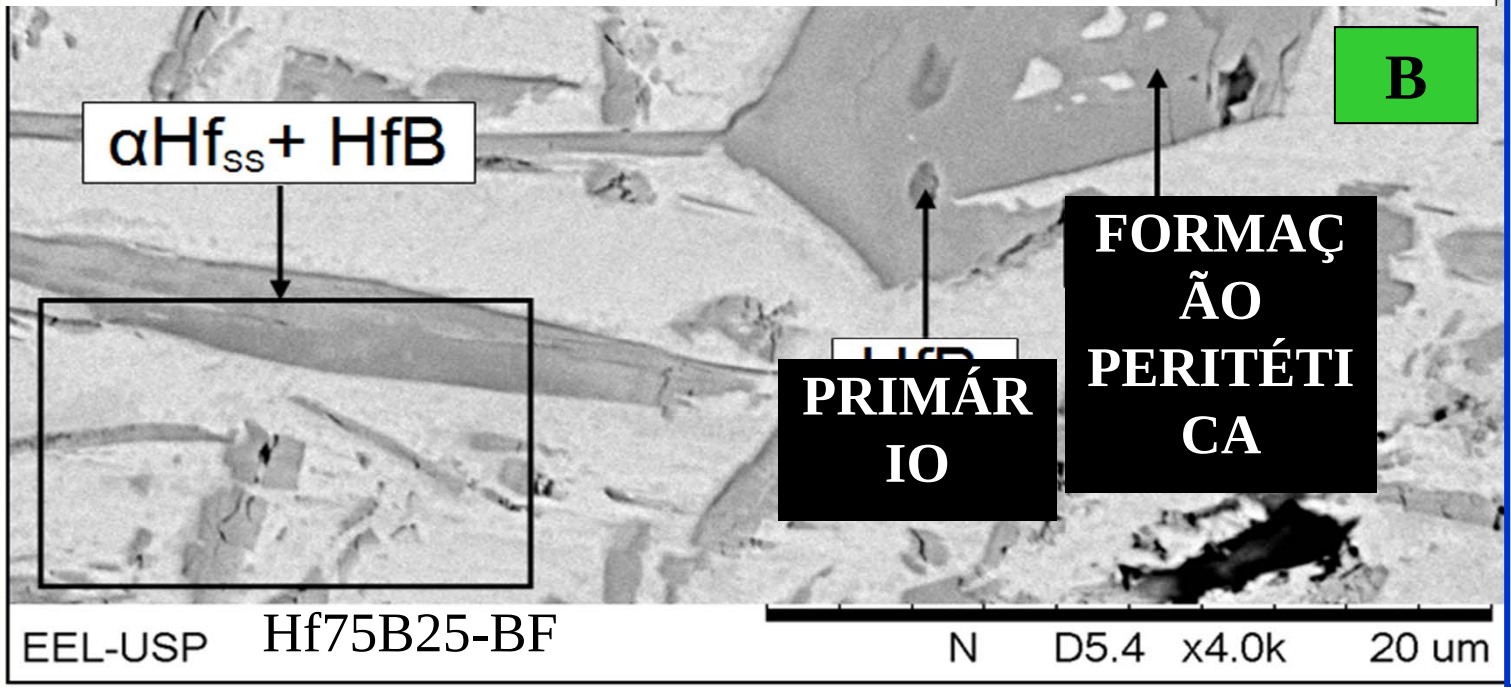

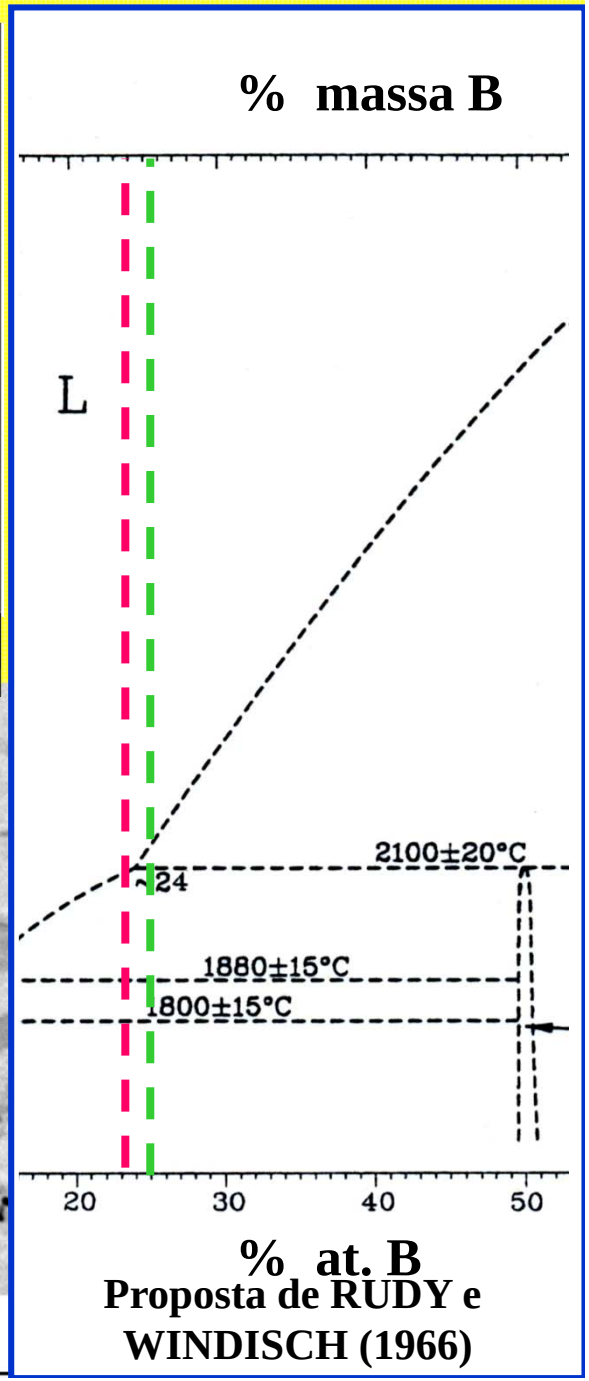

Proposta de RUDY e WINDISCH (1966)